CORROSION SCIENCE AND TECHNOLOGY, Vol.22, No.1(2023), pp.10~20 pISSN 1598-6462 / eISSN 2288-6524
[Research Paper] DOI: https://doi.org/10.14773/cst.2023.22.1.10

Corrosion Inhibition Screening of 2-((6-aminopyridin-2-yl)imino)indolin-3-one: Weight Loss, Morphology, and DFT Investigations

Nadia Betti[1] and Ahmed A. Al-Amiery[2,3,†]

[1]*Materials Engineering Department, University of Technology-Iraq, P.O. Box: 10001, Baghdad, Iraq*
[2]*Department of Chemical and Process Engineering, Universiti Kebangsaan Malaysia (UKM), P.O. Box: 43000, Bangi, Selangor.*
[3]*Energy and Renewable Energies Technology Center, University of Technology, Baghdad, 10001 Iraq.*
(Received July 12, 2022; Revised October 25, 2022; Accepted October 26, 2022)

Because of its inexpensive cost, mild steel is frequently employed as a construction material in different industries. Unfortunately, because of its limited resistance to corrosion, a protective layer must be applied to keep it from decaying in acidic or basic environments. The presence of heteroatoms, such as nitrogen, oxygen, and pi-electrons in the Schiff base could cause effective adsorption on the mild steel surface, preventing corrosion. The weight loss method and scanning electron microscopy (SEM) were used to investigate the inhibitory effects of APIDO on mild steel in a 1 M hydrochloric acid environment. The efficiency of inhibition increased as the inhibitor concentration increased and decreased as the temperature increased. The SEM analysis confirmed that the corrosion inhibition of APIDO proceeded by the formation of an organic protective layer over the mild steel surface by the adsorption process. Simulations based on the density functional theory are used to associate inhibitory efficacy with basic molecular characteristics. The findings acquired were compatible with the experimental information provided in the research.

Keywords: *Isatin, Schiff base, Mild steel, Corrosion inhibitor, DFT*

1. Introduction

Inhibitor application is among the most appropriate strategies for protecting alloys from corrosion, and it is becoming widely common around the world. Inhibitors were found in organic and inorganic compounds with functional groups containing heteroatoms (such as phosphorous, sulphur, oxygen and nitrogen), unsaturated bonds (such as double or triple bonds), and the planar conjugated structure, which includes all different types of aromatic rings that can provides effective electrons or empty orbitals to contribute electrons [1–10]. The first stage in the inhibiting action process is the adsorption of the organic inhibitors at the metallic environment interface. Organic compounds can adsorb on metallic surface via (a) electrostatic interactions between (-) charges with specially adsorbed anions (Cl) on the iron surface and the (+) charge of the inhibitor molecules. (b) Interactions of the inhibitor molecule's unshared electron pairs with d-orbital of iron atoms. (c) Association of the inhibitor molecule's electron with the iron, and/or (d) a combination of the abovementioned steps. Physisorption and chemisorption are two different types of interactions that characterize the adsorption of organic molecules on metallic surfaces. Both an electric charges surface on the metals and charged molecules on the solution phase are required for physisorption. Charge-transfer processes are involved in chemical adsorption. Although the corrosive solution contains chloride ions, hydrogen ions and water molecules, the inhibitor molecule (APIDO) is well absorbed on the metal surface. This can be described by the relative positions of different species. The number of interactions between the APIDO and iron orbital is determined by the nature of APIDO orbital. An efficient acceptor is a strong coordinating ligand like APIDO, which favors back bonding between the metal and the ligand. Cl, OH, and water molecules are weak acceptors, and no back bonding interaction with metal is expected, implying that APIDO (Fig. 1) is a more powerful adsorbent than the other molecules in the environment.

[†]Corresponding author: dr.ahmed1975@gmail.com, dr.ahmed1975@ukm.edu.my

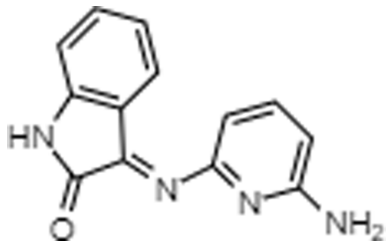

Fig. 1. The chemical structure of tested corrosion inhibitor

2. Experimental Section

2.1 Mild Steel Sampling

Mild steel coupons were used containing 0.21% carbon, 0.09% phosphorous, 0.05% manganese, 0.038% silicon, 0.01% aluminum, 0.05% sulfur and the rest iron. Before each experiment, the mild steel coupons were divided into different areas, cleaned with sandpaper, degreased with acetone, and dried in the oven before curing [11] to prevent the coupons from moisture in the air. The finished coupons were suspended by gage wire in a beaker containing 250 mL of 1 M HCl (37%) in the presence and absence of APIDO as the tested inhibitor. Each sample after corrosion assay was washed with distilled water, dipped in methyl alcohol to get rid of APIDO particles and chlorine residue, dipped in acetone, oven dried and finally re-weighed.

2.2 Weight Loss Measurements

Gravimetric analysis was performed on mild steel coupons in 1M HCl medium in the absence and presence of APIDO. The initial measurements of the polished coupons have been completed. The coupons were exposed to a solution of hydrochloric acid at a concentration of 1 M using a glass clamp in the presence and absence of APIDO at different concentrations of the inhibitor APIDO (0.0001, 0.0002, 0.0003, 0.0004, 0.0005, and 0.001 M). Vouchers were re-weighed after removal, rinsed with water and dried. The effect of time on inhibition efficiency was studied at different inhibitor concentrations for immersion periods (1, 5, 10, 24, 48 hours). The effect of temperature on damping efficiency was studied at different concentrations (0.0001 M to 0.001 M) at different temperatures (303, 313, 323 and 333 K) and for five hours of immersion. The temperature of the examined solution was regulated by the thermostat selector at the desired temperature. The values of corrosion rate (C_R; mm y^{-1}) and inhibiting efficiency (IE%) were determined using the equations. 1 and 2 individually [12].

$$C_R = \frac{87.6W}{DAT} \quad (1)$$

$$IE(\%) = \frac{C_{Ro} - C_R}{C_{Ro}} \quad (2)$$

where W is the weight loss, A is the exposure coupon area, D is the mild steel density, T is exposure time, C_{Ro} is the corrosion rates without APIDO and C_R corrosion rates with APIDO.

2.3 Surface Study

Mild steel coupons were immersed in inhibited and uninhibited acidic solutions and examined at room temperature by scanning electron microscopy (SEM). The difference in the surface of mild steel was examined by scanning electron microscope (TM1000 Hitachi Tabletop Microscope SEM). The tested coupon was exposed to 1 M HCl solution for 5 h without the inhibitor and in the presence of the inhibitor at a concentration of 0.0005 M. Furthermore, the investigated samples were taken, washed with deionized water, dried and examined by SEM.

2.4 Theoretical Investigations

Perhaps to explain the issue of inhibitor performance and to identify common important factors that may control inhibitory efficacy, here, we performed quantum chemical calculations. Theoretical factors were evaluated and confirmed by density function theory (DFT). To study the electronic properties of the investigated inhibitor molecules, a three-parameter hybrid Becke function was performed using the functional LYP binding function (B3LYP) [13,14]. The ionization energy and affinity were evaluated using the highest occupied molecular orbital (HOMO) and lowest unoccupied molecular (LUMO) and from which the electronegativity was determined [15].

$$\text{Ionization energy } (I) = -E_{HOMO} \quad (3)$$

$$\text{Electronic affinity (A)} = -E_{LUMO} \quad (4)$$

$$\text{Electronegativity } (\chi) = \frac{I + A}{2} \quad (5)$$

$$\text{Hardness } (\eta) = \frac{I - A}{2} \quad (6)$$

Transferred electrons fraction (ΔN) was determined [16] according to equation (7),

$$\Delta N = \frac{\phi - \chi_{inh}}{2(\eta_{Fe} + \eta_{inh})} \quad (7)$$

The iron work function (ϕ) was essentially taken as 4.82 eV, whereas the iron hardness was evaluated at 0 as $I = A$ [17].

3. Result and Discussion

3.1 Inhibitor Concentration Effect

The inhibitory activity increases with an increase in the concentration of the inhibitor. From Fig. 2, we note that there is a positive relationship between the concentration of the inhibitor and the inhibitory activity (Fig. 2). The increase in the concentration of the studied inhibitor leads to an increase in the adsorption of the inhibitor particles on the surface of mild steel as well as the surface coverage, and thus leads to a decrease in the corrosion rate. Experimental results indicate that the corrosion rate decreases with increasing concentration of the studied inhibitor [18,19].

3.2 Effect of Immersion Time

The obtained experimental results revealed that the exposure period has a significant influence on the values of the wear rate, weight loss, inhibitory effectiveness and the degree of surface coverage. Fig. 2 shows the relationship between wear rate, mass loss and inhibitory activity with exposure period to different concentrations of the inhibitor used. Fig. 2 also shows that the result of gravimetric measurements of the corrosion rate values decreases with the exposure period of the tested coupons to the acidic solution in the presence of the inhibitor. However, the corrosion rate value of the used inhibitor decreases with increasing concentration of the compound inhibitor, but it starts to increase when the exposure period is increased to 24 hours or more. Therefore, the increase in mass loss observed during the period of immersion in a solution of hydrochloric acid, prolonged and continuous. Moreover, Fig. 2 presents a plot of inhibitory efficacy versus time and also reveals the rate of wear over time. Experimental results showed that the inhibitory activity decreases with significantly increased immersion time for all concentrations of the tested inhibitor. The decrease in inhibitory activity with immersion time is attributed to the reaction of inhibitor molecules with ions in the solution resulting in inhibitor loss or depletion over time due to chemical reactions taking place within the acidic environment. The decrease in the inhibitory potency for a prolonged exposure time may be due to the lack of free inhibitor molecules in solution and thus the lack of metallic complex formation between the d-orbital of iron

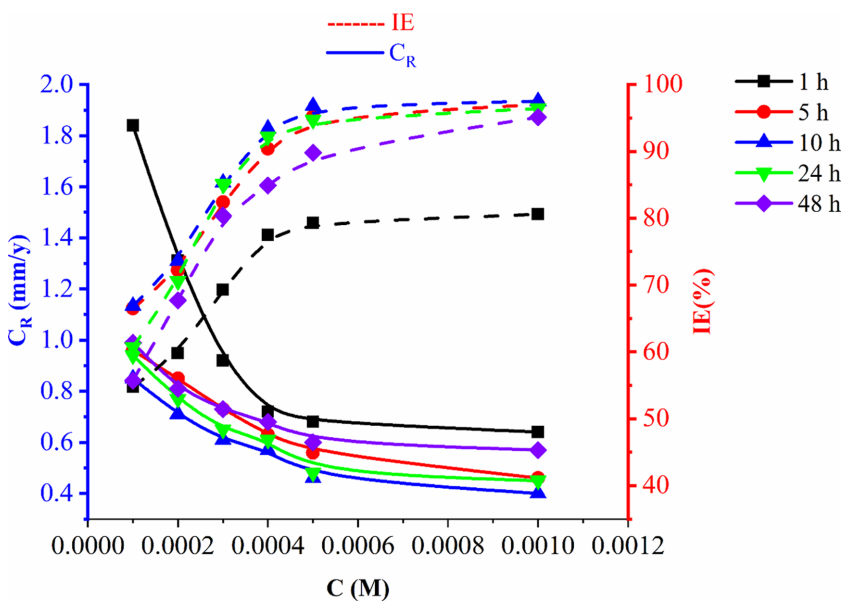

Fig. 2. Shows the effects of decreasing the weight of mild steel in 1.0 M HCl with increasing concentration of inhibitor at different immersion times and temperature of 303 K

atoms on the surface of mild steel and the unpaired pairs of inhibitor molecules electrons. Therefore, there may be a decrease in inhibitory efficacy with exposure period due to absorption. The highest inhibition activity was 95.2% after the immersion time (5 h), at a concentration of 0.0005 M of inhibitor, and increasing the concentration further did not lead to a marked difference in the inhibitory activity within the range of inhibitory concentration examined. This approximate stability of the inhibitory activity may be attributed to the saturation of the solution with inhibitor molecules at a concentration of 0.0005 M. It may also be due to the competing adsorption effect between the inhibitor molecules and the alloy surface which has been pre-treated with the initial film of the inhibitor molecules [20-24].

3.3 Impact of Temperature

The effect of temperature on the corrosion rate and inhibiting efficiency was studied. The achieved results were presented in Fig. 3. In general, it was observed that the value of the corrosion rate increases slightly with increasing temperature, as shown in Fig. 3. Also, increasing the temperature leads to an acceleration of the chemical reaction and a decrease in the solubility of oxygen, which in turn reduces the inhibition efficiency. Fig. 3 also shows the effect of the inhibitor and the negative effect of temperature on the inhibitory efficacy, whereby higher temperature leads to the accumulation of dynamic energy of the tested inhibitor molecules. The buildup of dynamic energy reduces the protective layer formed on the surface of the mild steel coupons. Besides at the highest studied temperature (333 K), the inhibition efficacy decreased from 95.2% to 87%. The decrease in inhibitory potency with increasing temperature at all concentrations indicates physisorption. Furthermore, desorption occurs at high temperatures, which results in the loss of inhibitor molecules from the coupon surface.

The inhibitory efficiency of APIDO is higher than that of certain chemical inhibitors documented in the literatures [26-36] for the concentration range under investigation; See Table 1. The target inhibitor APIDO shows significantly better inhibitory efficiency at very low doses compared to the previously examined synthetic organic corrosion inhibitors. In these examples in Table 1, for mild steel composite corrosion inhibitors in 1.0 HCl solution, a few of them also show remarkable inhibition performance at low concentrations. Of course, low concentration/high inhibition efficiency is not the only measure of the quality of inhibitors, non-toxic properties and simple and cost-effective synthesis process should also be considered. Thus, our compound inhibitor, synthesized from environmentally friendly materials, possesses great application potential as corrosion inhibitor for mild steel in acidic environments.

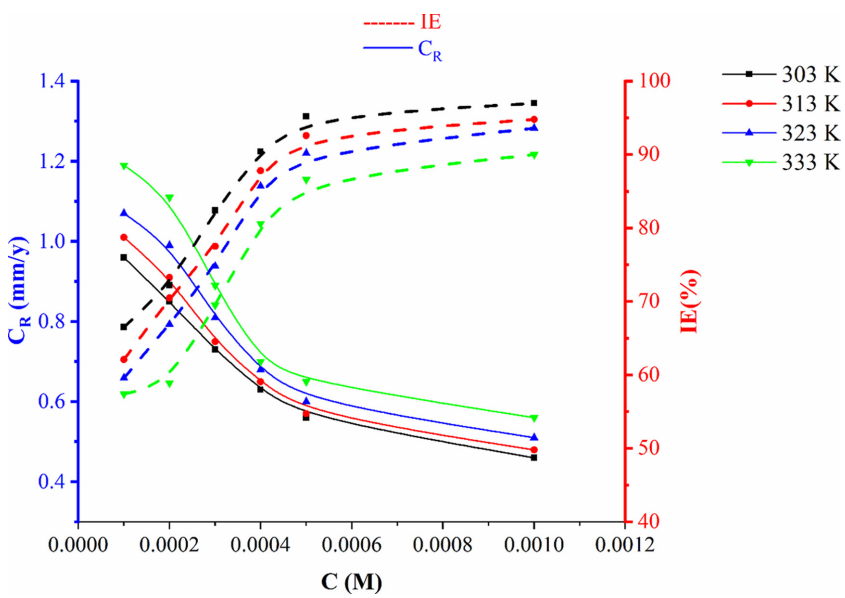

Fig. 3. Mild steel weight loss effects of in 1.0 M corrosive solution with different inhibitor concentrations at different temperatures for 5 h as immersion period

Table 1. Compares reported corrosion inhibitors to the one under investigation

Corrosion inhibitor.	Metal	Acid	IE%	Ref.
APIDO	Mild steel	HCl	95.2	-
3-(4-ethyl-5-mercapto-1, 2, 4-triazol-3-yl)-1-phenylpropanone (EMTP)	Mild steel	HCl	97	[26]
2-(4-phenyl-1H-1,2,3-triazol-1-yl) acetohydrazide	Mild steel	HCl	95.3	[27]
2-Amino-4-phenyl-N-benzylidene-5-(1,2,4-triazol-1-yl)thiazole	Mild steel	HCl	95	[27]
7-((1-benzyl-1H-1,2,3-triazol-4-yl)methyl)-1,3-dimethyl-3,7-dihydro-1H-purine-2,6–dione	Mild steel	HCl	91.7	[28]
7-((1-(4-fluorobenzyl)-1H-1,2,3-triazol-4-yl)methyl)-1,3-dimethyl-3,7-dihydro-1H-purine-2,6-dione	Mild steel	HCl	86.9	[28]
7-((1-(4-chlorobenzyl)-1H-1,2,3-triazol-4-yl)methyl)-1,3-dimethyl-3,7-dihydro-1H-purine-2,6-dione	Mild steel	HCl	94	[28]
7-((1-(4-bromobenzyl)-1H-1,2,3-triazol-4-yl)methyl)-1,3-dimethyl-3,7-dihydro-1H-purine-2,6-dione	Mild steel	HCl	91.8	[28]
7-((1-(4-iodobenzyl)-1H-1,2,3-triazol-4-yl)methyl)-1,3-dimethyl-3,7-dihydro-1H-purine-2,6-dione	Mild steel	HCl	90.9	[28]
5-methyl-4-((3-nitrobenzylidene) amino) -2,4-dihydro- 3H-1,2,4-triazole-3-thione	Mild steel	HCl	89.7	[29]
3-phenyl-4-amino-5-mercapto-1,2,4-triazole	Mild steel	HCl	97	[30]
2[5-(2-Pyridyl)-1,2,4-triazol-3-yl phenol	Mild steel	HCl	96.8	[31]
3,5-Bis(4-methyltiophenyl)-4H-1,2,4-triazole	Mild steel	HCl	93.5	[31]
3,5-Bis(4-pyridyl)-4H-1,2,4-triazole	Mild steel	HCl	89.1	[31]
3,5-Diphenyl-4H-1,2,4-triazole	Mild steel	HCl	82.8	[32]
3,5-Di(*m*-tolyl)-4-amino-1,2,4-triazole	Mild steel	HCl	95.8	[33]
5-Amino-1,2,4-triazole	Mild steel	HCl	24	[33]
5-Amino-3-mercapto-1,2,4-triazole	Mild steel	HCl	82	[33]
5-Amino-3-methyl thio-1,2,4-triazole	Mild steel	HCl	82	[33]
1-Amino-3-methyl thio-1,2,4-triazole	Mild steel	HCl	63	[34]
3-Benzylidene amino-1,2,4-triazole phosphonate	Mild steel	HCl	56.9	[34]
3-*p*-Nitro-benzylidene amino-1,2,4-triazole phosphonate	Mild steel	HCl	69.2	[34]
3-Salicylialidene amino-1,2,4-triazole phosphonate	Mild steel	HCl	43.2	[34]
3,5-Bis(methylene octadecyldimethylammonium chloride)-1,2,4-triazole	Mild steel	HCl	98.3	[35]
3-Amino-1,2,4-triazole-5-thiol	Mild steel	HCl	97.8	[36]

3.4 Adsorption Isotherm

A great deal of information is provided by using balanced adsorption models based on adsorption of inhibitor molecules onto the surface of mild steel. Given that the linear regression coefficient is very close to unity, the Langmuir isotherm was thought to be the most reliable method to confirm adsorption of the tested inhibitor on the surface of mild steel [34]. Based on relation (8), the Langmuir isothermal model is fully investigated.

$$\frac{C_{inh}}{\theta} = \frac{1}{K_{ads}} + C_{inh} \quad (8)$$

The above equation encapsulates the link between inhibitor concentration and surface coverage (θ). The area of the surface treated by a molecule of the investigated inhibitor is referred to as the surface coverage, and it may be calculated using equation (9).

$$\theta = \frac{w_o - w_i}{w_o} \quad (9)$$

When compared with other isothermal models, the C_{inh} vs. C_{inh} plot obtained at 303 K shows that the inhibitor molecules adhere to the Langmuir adsorption model more accurately. A higher K_{ads} value suggested better absorption and, ultimately, a more reliable process inhibition efficacy [35]. K_{ads} can be calculated using the intersection of the straight line (Fig. 4). The equation can be used to describe the relationship between the adsorption free energy and

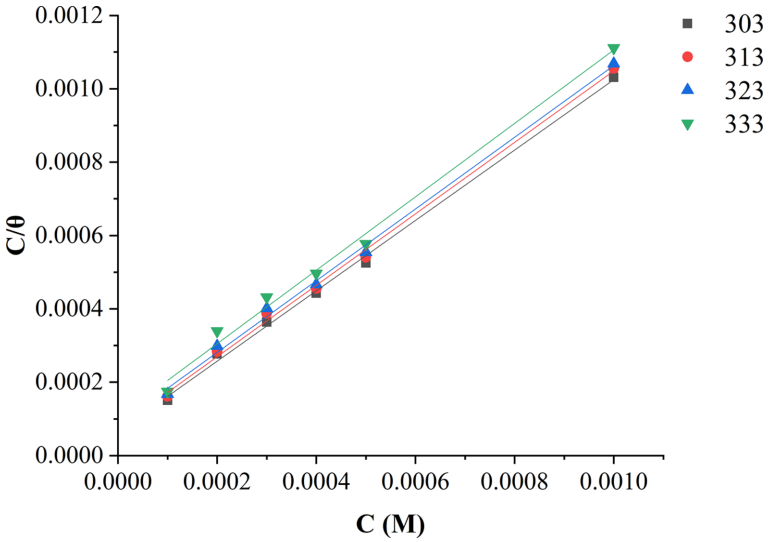

Fig. 4. Langmuir adsorption isotherms plots for the examined inhibitor molecules at various temperatures

the adsorption equilibrium constant (10).

$$\Delta G^{o}_{ads} = -RT\ln(55.5K_{ads}) \quad (10)$$

where R is gas constant, T is the absolute temperature, and K_{ads} is the equilibrium constant.

The inhibitor molecules are effectively adsorbed on the surface of the mild steel, according to the adsorption free energy (ΔG^{o}_{ads}), which has a negative value, indicating spontaneity in the adsorption process [36]. Obviously ($\Delta G^{o}_{ads} \leq -20$ kJ/mol) determines the adsorption of inhibitor molecules to the coupon surface. However, the exceptionally low adsorption free energy ($\Delta G^{o}_{ads} > -40$ kJ/mol) indicates chemical adsorption through coordination interactions between unoccupied iron atoms on the coupon surface and unpaired electron pairs in the studied inhibitor molecules [37]. In this example, the ΔG^{o}_{ads} value for the investigated inhibitor was found to be -38.7 kJ/mol. This means that the mechanism of inhibition refers to a mixed reaction type that includes chemisorption and physisorption.

3.5 Computational Studies

By analyzing the HOMO and LUMO molecular orbitals, the molecular interaction of the searched and identified inhibitor compound (MOs) was analyzed. The ability of inhibitory compound to donate electrons is related to HOMO energy. When the HOMO energy is high, the particle is more likely to donate electron pairs to a suitable acceptor element that possesses an open molecular orbital. In addition, the LUMO energy serves as a measure of a molecule's tendency to take an electron. It is important to note that molecules with lower LUMO energy values have a greater ability to receive electrons. The HOMO and LUMO molecular orbitals are believed to be closely related to the interaction of inhibitor molecules. Fig. 5 shows the frontier MO density distribution for the examined inhibitor molecule's ideal molecular structure, EHOMO, and ELUMO. Fig. 5 illustrates the results of the DFT analysis of the non-protonated inhibitor molecules to identify the ideal molecular structures, EHOMO and ELUMO. The HOMO populations gathered around the heterocyclic and aromatic rings in addition to -N=C- group, as seen in Fig. 5. Despite the fact that LUMO densities typically centered on the aromatic ring. The molecule with the high HOMO energy implies a more significant capacity to donate electrons to suitable elements have unfilled molecular orbitals with low energy and so characterizes the adsorption of inhibitor molecules on mild steel surface. The tendency to receive electrons is represented by the LUMO's energy. A high-energy HOMO may represent a tendency to donate an electron to a suitable element having a low-energy, vacant d-type orbital. Theoretical chemical properties such as HOMO and LUMO, energy gap (E = HOMO-LUMO), hardness, ductility, electronegativity,

and affinity are important and useful metrics for relating the corrosion inhibitory effectiveness of inhibitor molecules. Table 2 shows the quantitative chemical parameters calculated for the assessed inhibitor. Table 2 shows that APIDO molecules have a high HOMO energy value. This indicates that APIDO molecules have a high ability to endow electron pairs. This supports the experimental results showing that APIDO and iron atoms interact at the surface by forming coordination bonds. LUMO energy measures the bonds of electrons and indicates how vulnerable a molecule is to nucleophilic attack. The lower value energy has a stronger ability to receive an electron in LUMO. Low energy gap (ΔE) values provide good inhibitory efficacy because it reduces the excitation energy required to remove the electron from the orbital [30]. The chemical softness was also evaluated, and the chemical hardness was calculated as the energy gap/2. These properties are shown in Table 2 with information regarding the reactive performance of the molecule. A soft molecule is one that has a lower E value because it is more polarizable and is usually associated with high chemical reactivity and low dynamic stability [31,32]. Adsorption of the inhibitor molecules occurs on the skate of the metal at the highest fineness and at the lowest hardness. The calculated results show that APIDO particles have low values of E and hardness, which is consistent with the laboratory results showing that APIDO particles may have significant inhibitory activity on the surface of mild steel via a physisorption (electrostatic interaction) adsorption mechanism. Because HOMO has high energy value and best ability to give off electrons, APIDO molecules showed significant inhibitory effect. In addition, this is an exact match with the (ΔG^{o}_{ads}) value determined using adsorption isotherms. By controlling the electron density in the active site, the structure of the molecule can influence the adsorption. Usually, places with a negative charge on the particles are where the electrophilic attacks occur. The electron density was centered on each molecule as well as the oxygen and nitrogen atoms, as shown in Fig. 5. Electric vehicles frequently attack places with higher electron density. In order to have the strongest bonding to the steel surface, the oxygen and nitrogen atoms were the active sites. The ability of an inhibitor to inhibit is predicted by its electronegativity. The equation was used to calculate the number of electrons exchanged between the molecules of the element and the inhibitor illustrated by equation (7), that as the electronegativity of the inhibitor rises, so does the electron transfer capacity between the elements and molecules. When an electron is transferred between a steel surface and an inhibitor molecule, the electronegativities remain constant and are compatible. The quantity of electrons transported from the inhibitor molecules to the iron atoms' d-orbital on the coupon surface was used to measure the acceptor-donor interactions. The APIDO is typically followed when ΔN has a positive value, which indicates the inhibitor molecule's ability to donate its electrons, and vice versa for a negative one [14,18].

Table 2. Quantum parameters for APIDO molecules

Inhibitor	Values
$I\,(eV)$	9.427
$V\,(eV)$	4.832
$E_{HOMO}\,(eV)$	-9.427
$E_{LOMO}\,(eV)$	-4.832
$\Delta E\,(eV)$	-4.595
χ	-7.1295
η	-2.2975
ΔN	-2.6

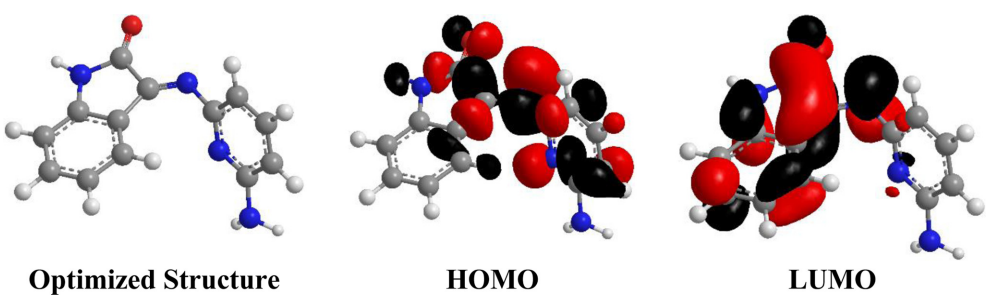

Fig. 5. APIDO molecular optimized electronic structures (HOMO and LUMO)

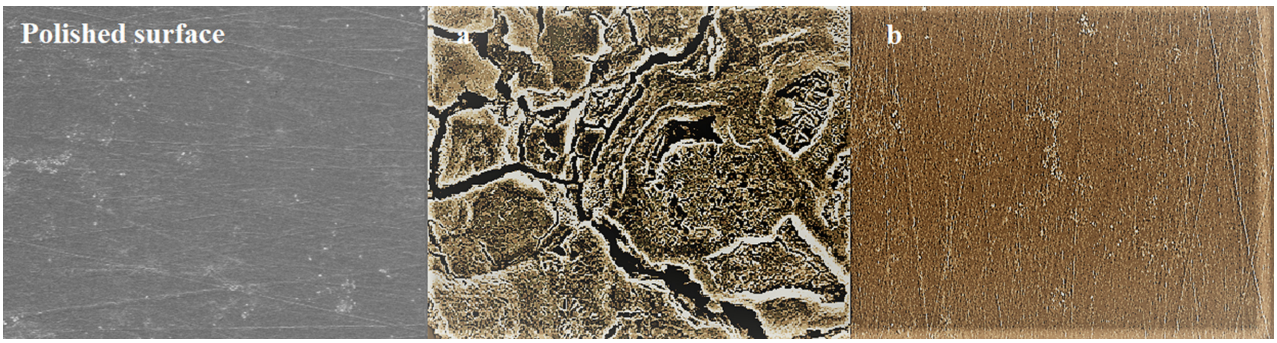

Fig. 6. SEM was imaged for mild steel in 1 M HCl solution for 5 h (a) without and (b) with APIDO comparable with the polished surface

3.6 Surface Analysis

Figs. 6a and 6b show the differences seen on the surface of the tested coupon after an exposure time of 5 h in 1 M HCl without and with addition of APIDO. Without an inhibitor, it is noted that the surface of the coupon exposed to the hydrochloric acid solution contains surface holes caused by the corrosion caused by the acid solution. In the presence of APIDO in the acidic solution, the corrosion effect is absent from the coupon surface (Fig. 6b). It is observed that the surface of the tested coupon treated with APIDO when immersed in the corrosive solution is quite comparable with the polished surface (Fig. 6). This indicates that the protective coating of the steel surface of the inhibitor particles acts as a defense against the attack of the corrosive solution.

3.7 The corrosion inhibition mechanism described

The coupon substrate exhibits negative charges in the presence of HCl solution due to the particular adsorption of chloride ions on the coupon substrate shown in relation (11).

$$Fe + Cl^{-} \leftrightarrow (FeCl^{-})_{ads} \quad (11)$$

Because of the high electron density on the heteroatoms of the tested inhibitor, protonation of these heteroatoms is straightforward, resulting in positive charges on inhibitor molecules, as seen in Fig. 7. Physical adsorption can occur as a result of physical interactions between positive charges on inhibitor species and negative charges on a mild steel surface. Furthermore, coordinating bonds generated on the steel substrate between unpaid electrons of heteroatoms of studied inhibitor molecules and vacant d-orbitals of metal atom [8,9].

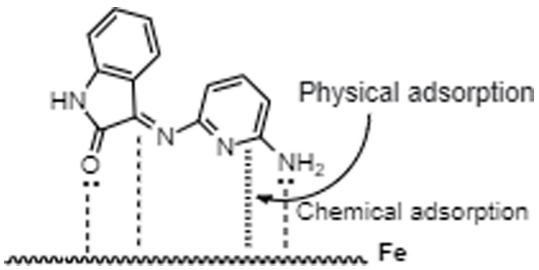

Fig. 7. The proposed protection corrosion mechanism of APIDO for mild steel

4. Conclusions

On the surface of the coupon, in 1 M HCl, experiments were performed to prevent mild steel surface corrosion and to adsorb the newly synthesized inhibitor on the surface. The result shows the following:

As the concentration of the tested inhibitor increases, the mild steel surface in 1 M hydrochloric acid solution becomes more effective against the corrosive solution. For 0.0005 M of the tested inhibitor, the highest inhibition efficacy of 95.2% was achieved. The development of a protective layer at the metal/electrolyte interface was discovered to be the cause of this behavior.

According to weight loss methods, the higher temperature of the solution will reduce the inhibition efficacy.

The adsorption process was obeyed Langmuir adsorption isotherm model. A negative Gads value indicates that the mechanism of adsorption follows the chemical and physical adsorption isotherm process.

The SEM analysis confirms that the corrosion inhibition of APIDO was proceeded by forming an organic protective layer over the mild steel surface by means of the adsorption process.

All experimental results were very consistent with theoretical studies. The relationship between the inhibitory potency and the molecular structure of the tested inhibitor was effectively explained by DFT.

As a result, general conclusions are based on the effectiveness of the tested inhibitor in acting as a corrosion inhibitor for mild steel in a hydrochloric acid solution.

References

1. T. A. Salman, A. A. Al-Amiery, L. M. Shaker, A. A. Kadhum, M. S. Takriff, A study on the inhibition of mild steel corrosion in hydrochloric acid environment by 4-methyl-2-(pyridin-3-yl) thiazole-5-carbohydrazide, *The International Journal of Corrosion and Scale Inhibition*, **8**, 1035 (2019). Doi: https://doi.org/10.17675/2305-6894-2019-8-4-14
2. H. J. Habeeb, H. M. Luaibi, T. A. Abdullah, R. M. Dakhil, R. M. Kadhum, A. A. Al-Amiery, Case study on thermal impact of novel corrosion inhibitor on mild steel, *Case Studies in Thermal Engineering*, **12**, 64 (2018). Doi: https://doi.org/10.1016/j.csite.2018.03.005
3. T. A. Salman, Q. A. Jawad, M. A. Hussain, A. A. Al-Amiery, L. Mohamed, A. A. Kadhum, M. S. Takriff, Novel ecofriendly corrosion inhibition of mild steel in strong acid environment: Adsorption studies and thermal effects, *The International Journal of Corrosion and Scale Inhibition,* **8**, 1123 (2019). Doi: https://doi.org/10.17675/2305-6894-2019-8-4-19
4. A. A. Alamiery, W. N. Wan Isahak, M. S. Takriff, Inhibition of Mild Steel Corrosion by 4-benzyl-1-(4-oxo-4-phenylbutanoyl) thiosemicarbazide: Gravimetrical, Adsorption and Theoretical Studies, *Lubricants*, **9**, 93 (2021). Doi: https://doi.org/10.3390/lubricants9090093
5. D. M. Jamil, A. K. Al-Okbi, M. M. Hanon, K. S. Rida, A. F. Alkaim, A. A. Al-Amiery, A. Kadhim, A. A. Kadhum, Carbethoxythiazole corrosion inhibitor: As an experimentally model and DFT theory, *Jounal of Engineering and Applied Science*, **13**, 3952 (2018). Doi: https://doi.org/10.36478/jeasci.2018.3952.3959
6. A. Y. Musa, W. Ahmoda, A. A. Al-Amiery, A. A. Kadhum, A. B. Mohamad, Quantum chemical calculation for the inhibitory effect of compounds, *Journal of Structural Chemistry*, **54**, 301 (2013). Doi: https://doi.org/10.1134/S0022476613020042
7. S. Al-Baghdadi, T. S. Gaaz, A. Al-Adili, A. A. Al-Amiery, M. S. Takriff, Experimental studies on corrosion inhibition performance of acetylthiophene thiosemicarbazone for mild steel in HCl complemented with DFT investigation, *International Journal Low-Carbon Technology*, **16**, 181 (2021). Doi: https://doi.org/10.1093/ijlct/ctaa050
8. A. Al-Amiery, T. A. Salman, K. F. Alazawi, L. M. Shaker, A. A. Kadhum, M. S. Takriff, Quantum chemical elucidation on corrosion inhibition efficiency of Schiff base: DFT investigations supported by weight loss and SEM techniques, *International Journal Low-Carbon Technology*, **15**, 202 (2020). Doi: https://doi.org/10.1093/ijlct/ctz074
9. T. A. Salman, K. F. Al-Azawi, I. M. Mohammed, S. B. Al-Baghdadi, A. A. Al-Amiery, T. S. Gaaz, A. A. Kadhum, Experimental studies on inhibition of mild steel corrosion by novel synthesized inhibitor complemented with quantum chemical calculations, *Results in Physics*, **10**, 291 (2018). Doi: https://doi.org/10.1016/j.rinp.2018.06.019
10. D. S. Zinad, M. Hanoon, R. D. Salim, S. I. Ibrahim, A. A. Al-Amiery, M. S. Takriff, A. A. Kadhum, A new synthesized coumarin-derived Schiff base as a corrosion inhibitor of mild steel surface in HCl medium: Gravimetric and DFT studies, *The International Journal of Corrosion and Scale Inhibition*, **9**, 228 (2020). Doi: https://doi.org/10.17675/2305-6894-2020-9-1-14
11. A. A. Alamiery, Effect of Temperature on the Corrosion Inhibition of 4-ethyl-1-(4-oxo-4-phenylbutanoyl)thiosemicarbazide on Mild Steel in HCl Solution, *Letters in Applied NanoBioScience*, **11**, 3502 (2022). Doi: https://doi.org/10.33263/LIANBS112.35023508
12. ASTM G1, Standard Practice for Preparing, Cleaning, and Evaluating Corrosion Test, pp. 1 – 9, ASTM International (2011). Doi: http://dx.doi.org/10.1520/G0001-03R11
13. D. S. Zinad, Q. A. Jawad, M. A. Hussain, A. Mahal, L. Mohamed, A. A. Al-Amiery, Adsorption, temperature and corrosion inhibition studies of a coumarin derivatives corrosion inhibitor for mild steel in acidic medium: Gravimetric and theoretical investigations, *International Journal of Corrosion and Scale Inhibition*, **9**, 134 (2020). Doi: https://doi.org/10.17675/2305-6894-2020-9-1-8
14. J. A. Yamin, E. A. Sheet, A. Al-Amiery, Statistical analysis and optimization of the corrosion inhibition efficiency of a locally made corrosion inhibitor under different operating variables using RSM, *International Journal of Corrosion and Scale Inhibiton*, **9**, 502 (2020). Doi: http://doi.org/10.17675/2305-6894-2020-9-2-6

15. T. A. Salman, D. S. Zinad, S. H. Jaber, M. Al-Ghezi, A. Mahal, M. S. Takriff, A. A. Al-Amiery, Effect of 1, 3, 4-thiadiazole scaffold on the corrosion inhibition of mild steel in acidic medium: An experimental and computational study, *Journal Bio-and Tribo-Corrosion*, **5**, 11 (2019). Doi: https://doi.org/10.1007/s40735-019-0243-7
16. T. Koopmans Ordering of wave functions and eigenenergies to the individual electrons of an atom. Physica, **1**, 104 (1933). Doi: https://doi.org/10.1016/S0031-8914(34)90011-2
17. S. B. Al-Baghdadi, A. A. Al-Amiery, A. A. Kadhum, M. S. Takriff, Computational Calculations, Gravimetrical, and Surface Morphological Investigations of Corrosion Inhibition Effect of Triazole Derivative on Mild Steel in HCl, *Journal of Computational and Theoretical Nanoscience*, **17**, 2897 (2020). Doi: https://doi.org/10.1166/jctn.2020.9328
18. M. M. Hanoon, Z. A. Gbashi, A. A. Al-Amiery, A. Kadhim, A. A. Kadhum, M. S. Takriff, Study of Corrosion Behavior of N'-acetyl-4-pyrrol-1-ylbenzohydrazide for Low-Carbon Steel in the Acid Environment: Experimental, Adsorption Mechanism, Surface Investigation, and DFT Studies, *Progress in Color Colorants and Coatings*, **15**, 133 (2022). Doi: https://dx.doi.org/10.30509/PCCC.2021.166836.1118
19. M. M. Hanoon, A. M. Resen, A. A. Al-Amiery, A. A. Kadhum, M. S. Takriff, Theoretical and Experimental Studies on the Corrosion Inhibition Potentials of 2-((6-Methyl-2-Ketoquinolin-3-yl) Methylene) Hydrazinecarbothioamide for Mild Steel in 1 M HCl, *Progress in Color Colorants and Coatings*, **15**, 11 (2022). Doi: https://dx.doi.org/10.30509/PCCC.2020.166739.1095
20. A. A. Al-Amiery, W. K. Al-Azzawi, W. N. R. W. Isahak, Isatin Schiff base is an effective corrosion inhibitor for mild steel in hydrochloric acid solution: gravimetrical, electrochemical, and computational investigation, *Scientific Reports*, **12**, 17773 (2022). Doi: https://doi.org/10.1038/s41598-022-22611-4
21. N. Betti, A. A. Al-Amiery, W. K. Al-Azzawi, Experimental and Quantum Chemical Investigations on the Anticorrosion Efficiency of a Nicotinehydrazide Derivative for Mild Steel in HCl, *Molecules*, **27**, 6254 (2022). Doi: https://doi.org/10.3390/molecules27196254
22. B. S. Mahdi, M. K. Abbass, M. K. Mohsin, W. K. Al-azzawi, M. M. Hanoon, M. H. H. Al-kaabi, L. M. Shaker, A. A. Al-amiery, W. N. R. W. Isahak, A. A. H. Kadhum, M. S. Takriff, Corrosion Inhibition of Mild Steel in Hydrochloric Acid Environment Using Terephthaldehyde Based on Schiff Base: Gravimetric, Thermodynamic, and Computational Studies, *Molecules*, **27**, 4857 (2022). Doi: https://doi.org/10.3390/molecules27154857
23. I. A. A. Aziz, M. H. Abdulkareem, I. A. Annon, M. M. Hanoon, M. H. H. Al-Kaabi, L. M. Shaker, A. A. Alamiery, W. N. R. W. Isahak, M. S. Takriff, Weight Loss, Thermodynamics, SEM, and Electrochemical Studies on N-2-Methylbenzylidene-4-antipyrineamine as an Inhibitor for Mild Steel Corrosion in Hydrochloric Acid, *Lubricants*, **10**, 23 (2022). Doi: https://doi.org/10.3390/lubricants10020023
24. I. A. Alkadir Aziz, I. A. Annon, M. H. Abdulkareem, M. M.Hanoon, M. H. Alkaabi, L. M. Shaker, A. A. Alamiery, W. N. R. Wan Isahak, M. S. Takriff, Insights into Corrosion Inhibition Behavior of a 5-Mercapto-1, 2, 4-triazole Derivative for Mild Steel in Hydrochloric Acid Solution: Experimental and DFT Studies, *Lubricants*, **9**, 122 (2021). Doi: https://doi.org/10.3390/lubricants9120122
25. A. A. Alamiery, W. N. R. Wan Isahak, M. S. Takriff, Inhibition of Mild Steel Corrosion by 4-benzyl-1-(4-oxo-4-phenylbutanoyl)thiosemicarbazide: Gravimetrical, Adsorption and Theoretical Studies, *Lubricants*, **9**, 93 (2021). Doi: https://doi.org/10.3390/lubricants9090093
26. A. Alamiery, Corrosion inhibition effect of 2-N-phenylamino-5-(3-phenyl-3-oxo-1-propyl)-1, 3, 4-oxadiazole on mild steel in 1 M hydrochloric acid medium: Insight from gravimetric and DFT investigations, *Materials Science for Energy Technologies*, **4**, 398 (2021). Doi: https://doi.org/10.1016/j.mset.2021.09.002
27. A. A. Alamiery, Anticorrosion effect of thiosemicarbazide derivative on mild steel in 1 M hydrochloric acid and 0.5 M sulfuric Acid: Gravimetrical and theoretical studies. *Materials Science for Energy Technologies,* **4**, 263 (2021). Doi: https://doi.org/10.1016/j.mset.2021.07.004
28. I. Aziz, I. Annon, M. H. Abdulkareem, M. M. Hanoon, M. H. Alkaabi, L. M. Shaker, A. A. Alamiery, W. N. R. Wan Isahak, and M. S. Takriff, Insights into Corrosion Inhibition Behavior of a 5-Mercapto-1, 2, 4-triazole Derivative for Mild Steel in Hydrochloric Acid Solution: Experimental and DFT Studies, *Lubricants*, **9**, 122 (2021). Doi: https://doi.org/10.3390/lubricants9120122
29. A. Nahlé, R. Salim, F. El Hajjaji, M. R. Aouad, M. Messali, E. Ech-Chihbi, B. Hammouti, M. Taleb, Novel triazole derivatives as ecological corrosion inhibitors for mild steel in 1.0 M HCl: Experimental & theoretical approach, *RSC Advances*, **11**, 4147 (2021). Doi: https://doi.org/10.1039/D0RA09679B

30. A. Espinoza-Vázquez, F. J. Rodríguez-Gómez, I. K. Martínez-Cruz, D. Ángeles-Beltrán, G. E. Negrón-Silva, M. Palomar-Pardavé, L. L. Romero, D. Pérez-Martínez, A. M. Navarrete-López, Adsorption and corrosion inhibition behaviour of new theophylline–triazole-based derivatives for steel in acidic medium, *Royal Society Open Science*, **6**, 181738 (2019). Doi: https://doi.org/10.1098/rsos.181738
31. I. Merimi, R. Benkaddour, H. Lgaz, N. Rezki, M. Messali, F. Jeffali, H. Oudda, B. Hammouti, Insights into corrosion inhibition behavior of a triazole derivative for mild steel in hydrochloric acid solution, *Materials Today Proceedings*, **13**, 1008 (2019). Doi: https://doi.org/10.1016/j.matpr.2019.04.066
32. L. Wang, M. J. Zhu, F. C. Yang, C. W. Gao, Study of a triazole derivative as corrosion inhibitor for mild steel in phosphoric acid solution, *International Journal of Corrosion*, **2012**, 573964 (2012). Doi: https://doi.org/10.1155/2012/573964
33. F. Bentiss, M. Bouanis, B. Mernari, M. Traisnel, H. Vezin, M. Lagrenee, Understanding the adsorption of 4H-1, 2, 4-triazole derivatives on mild steel surface in molar hydrochloric acid, *Applied Surface Science*, **253**, 3696 (2007). Doi: https://doi.org/10.1016/j.apsusc.2006.08.001
34. B. El Mehdi, B. Mernari, M. Traisnel, F. Bentiss, M. Lagrenee, Synthesis and comparative study of the inhibitive effect of some new triazole derivatives towards corrosion of mild steel in hydrochloric acid solution, *Materials Chemistry and Physics*, **77**, 489 (2003). Doi: https://doi.org/10.1016/S0254-0584(02)00085-8
35. H. H Hassan, E. Abdelghani, M. A. Amin, Inhibition of mild steel corrosion in hydrochloric acid solution by triazole derivatives: Part I. Polariztion and EIS Studies, *Electrochimica Acta*, **52**, 6359 (2007). Doi: https://doi.org/10.1016/j.electacta.2007.04.046
36. S. Ramesh, S. Rajeswari, Corrosion inhibition of mild steel in neutral aqueous solution by new triazole derivatives, *Electrochimica Acta*, **49**, 811 (2004). Doi: https://doi.org/10.1016/j.electacta.2003.09.035